

Intercalibration of Passive Microwave Rain Rates

Kyle Hilburn and Frank Wentz
 Email: hilburn@remss.com

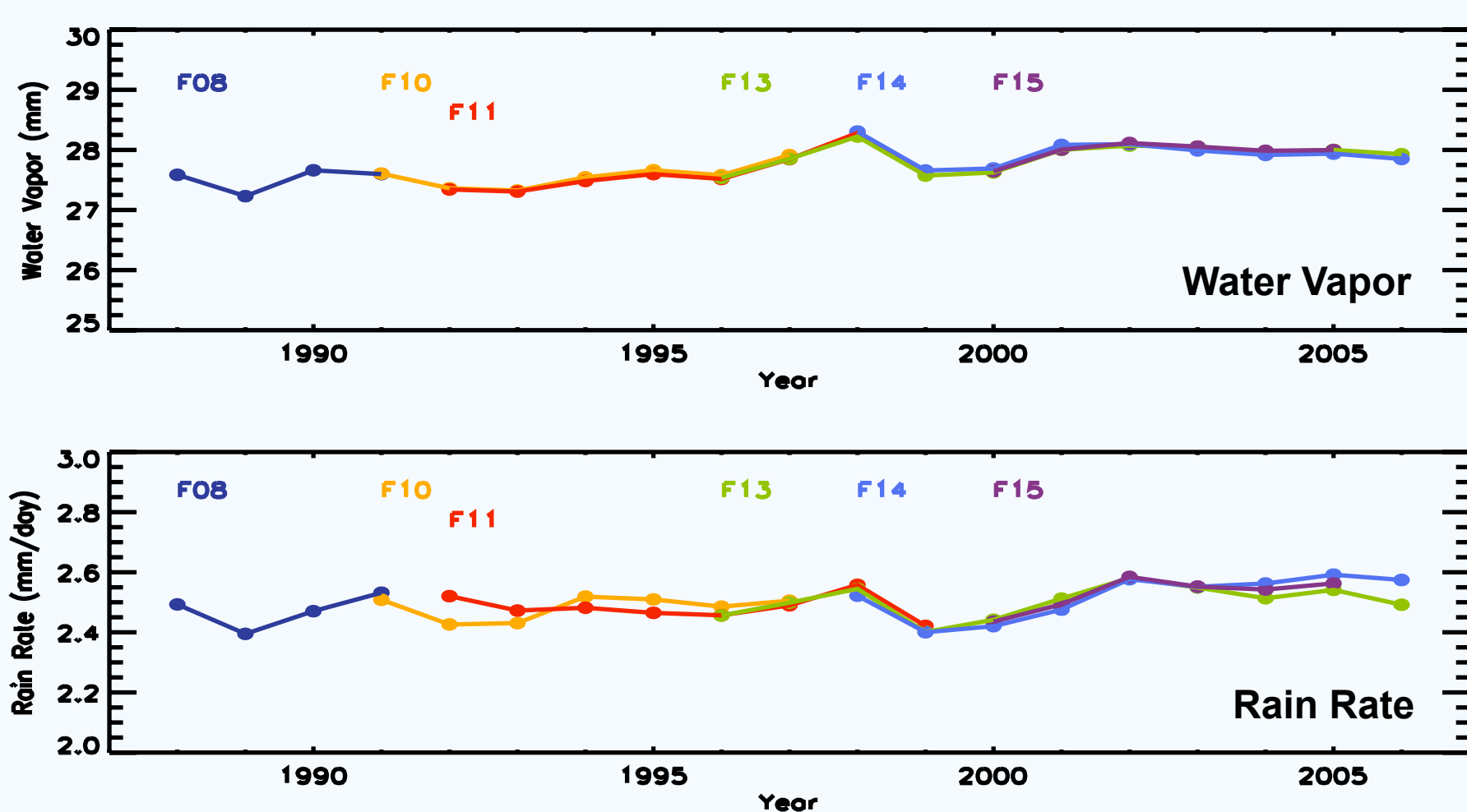
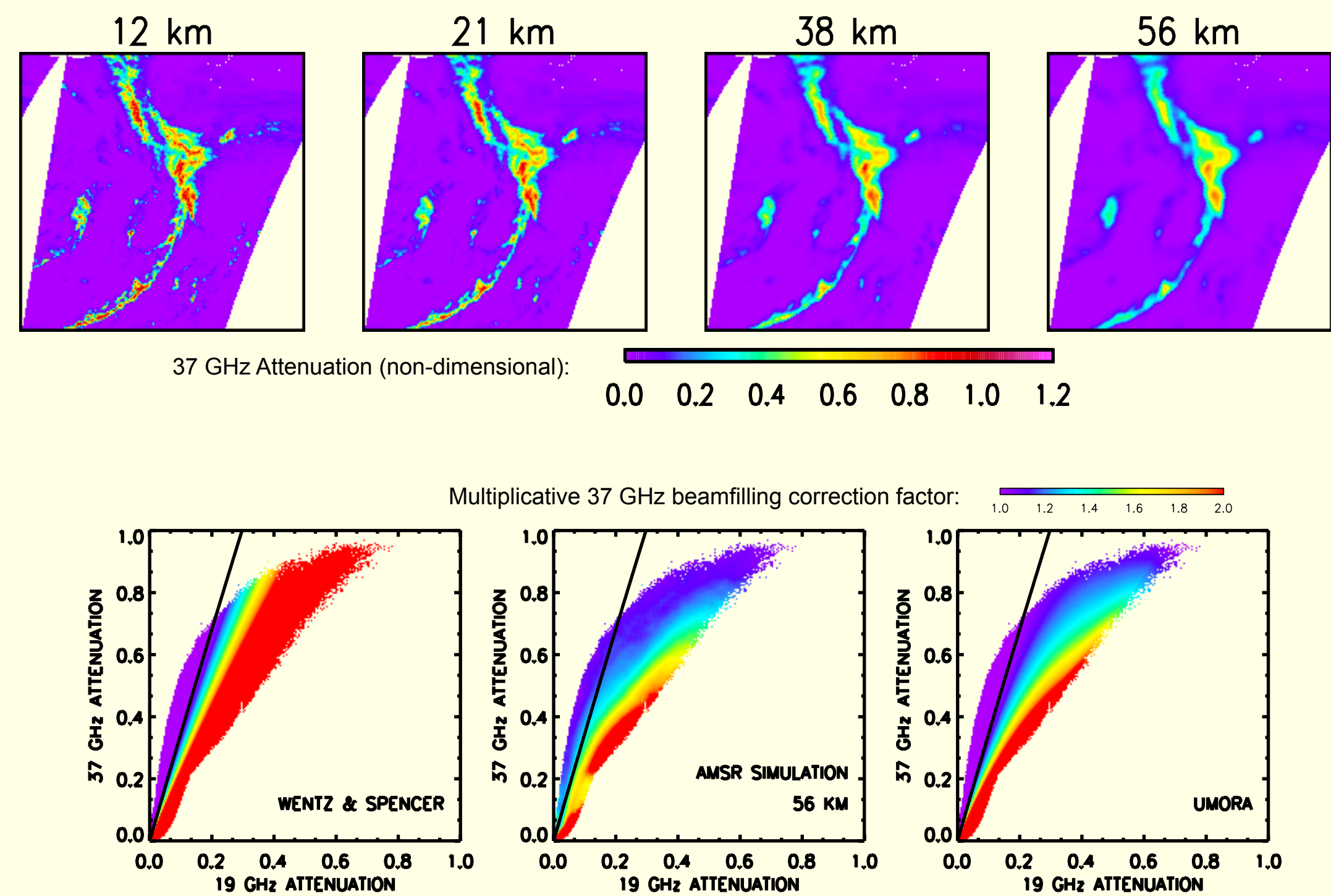
Remote Sensing Systems
 www.remss.com

Algorithm Improvements

The Unified Microwave Ocean Retrieval Algorithm (UMORA) simultaneously retrieves SST, surface wind, water vapor, cloud water, and rain rate from SSM/I, TMI, and AMSR-E. The rain component of UMORA is based on Wentz and Spencer (1998), but has recently been improved. Improvements include new rain column heights and a new beamfilling correction. The new beamfilling correction is a function of both the sensor resolution and the ratio of the 19 and 37 GHz attenuation values. Further information about algorithm improvements is available from Kyle (hilburn@remss.com).

(TOP) Resolution dependence was quantified using optimal interpolation to artificially resample ASMR-E brightness temperatures from their original 12 km resolution down to 21, 38, and 56 km. This example has scene average attenuation values of 1.17, 0.95, 0.86 and 0.79. Thus, not only does the pattern become smoother, but is biased lower. This biasing is the beamfilling effect.

(BOTTOM) The Wentz and Spencer beamfilling correction (left) assumed that the variability of liquid in the footprint was spatially distributed following a gamma distribution. The AMSR-E simulation (middle) shows that as 37 GHz attenuation increases above 0.6, large departures from the theoretical Mie ratio (black line) do not imply large beamfilling corrections because of sensor saturation. The UMORA correction (right) is based on a gamma distribution but it also models saturation. It matches the simulated data much better than Wentz and Spencer.



Agreement Among Satellites

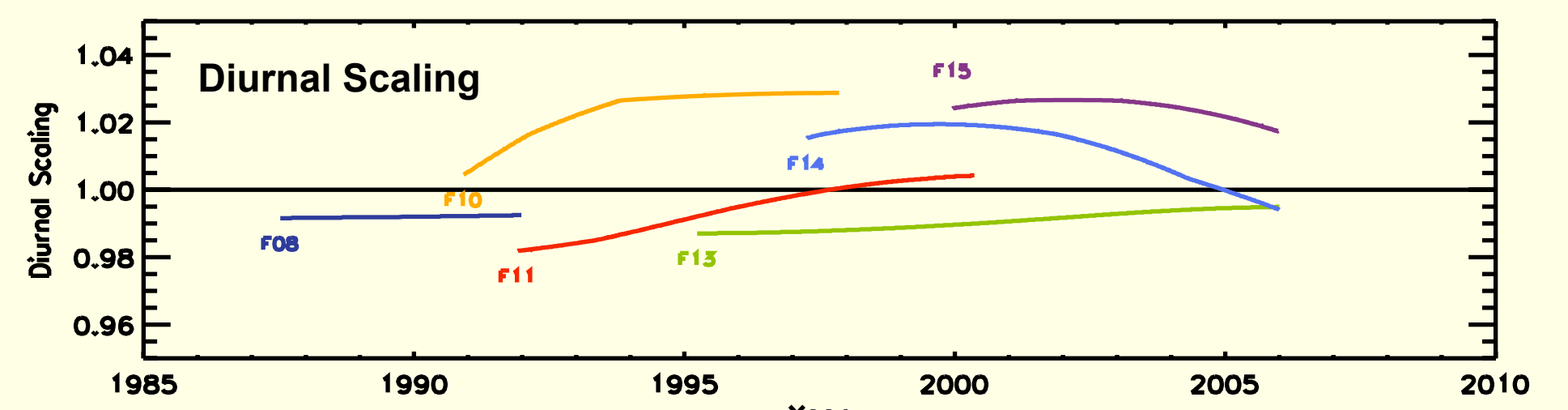
(TOP) UMORA estimates of water vapor from the SSM/I agree very well. In the most recent Version 6, the six SSM/I are calibrated to a precision of about 0.1 K in brightness temperature. Our wind speed retrievals, which are very sensitive to brightness temperature calibration errors, are in good agreement indicative of intercalibration errors of 0.1 K or less.

(BOTTOM) UMORA estimates of rain rate are well calibrated. The scaling adjustments described below have been applied. About half of the intersatellite disagreement is due to real geophysical time-of-day effects for rain rate. The other half (less than 3%) has yet to be explained. The remaining discrepancy may be due to nonlinearity in the calibration equation; or it may be a multiplicative error (which becomes large at the temperatures of rain scenes) arising from small errors in spillover or hot load specification.

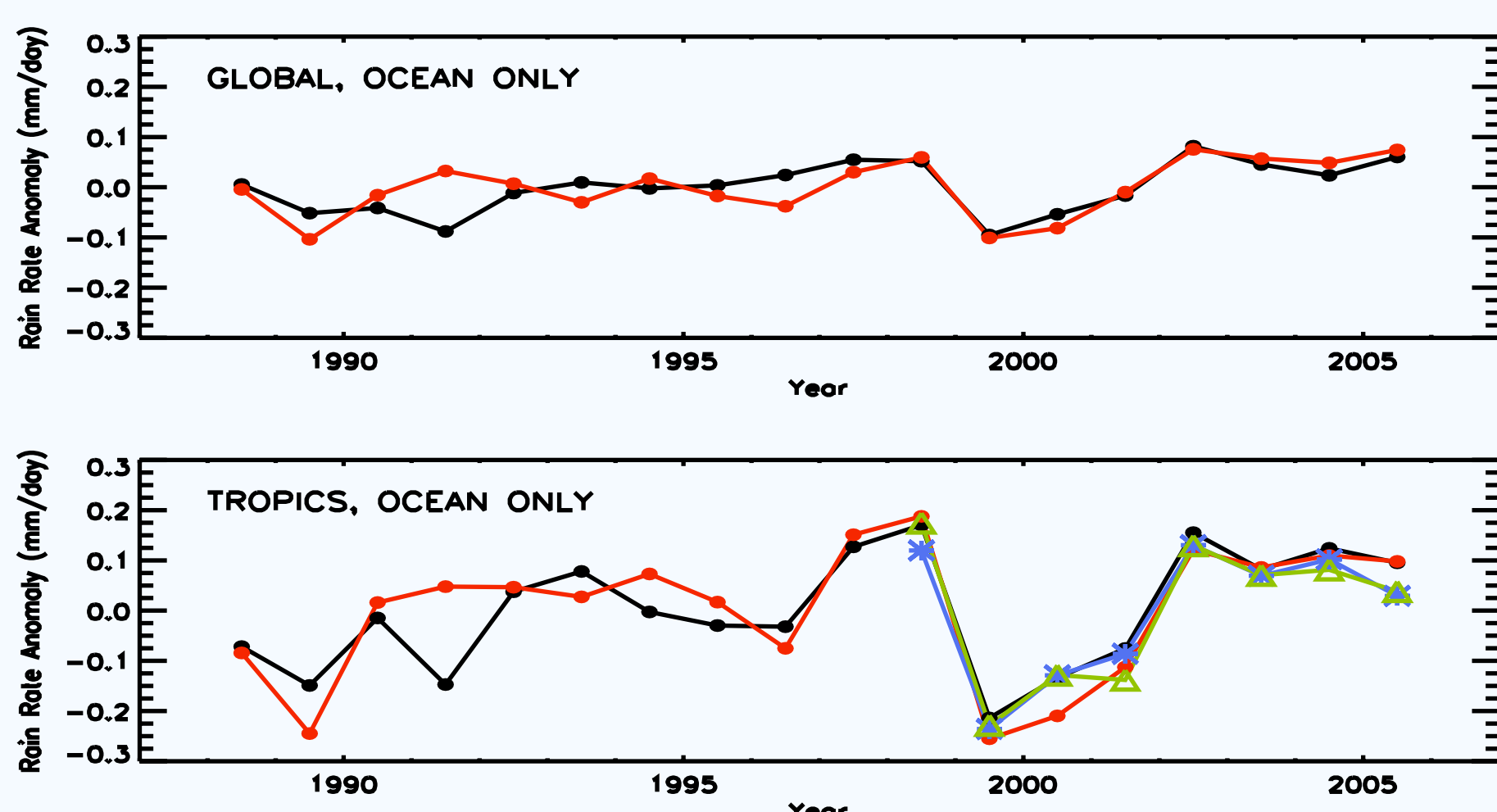
Time-of-Day Effects

(TOP) Diurnal corrections implied by the SSM/I local equatorial crossing times and TMI diurnal cycle. While the TMI diurnal cycle of rain has a strong first harmonic, the evening trough is flatter than the morning peak, leading to systematic biases. Note that in general, late morning satellites (F10, F14, and F15) have adjustments that increase the average, whereas early morning satellites (F08, F11, and F13) have adjustments that decrease the average.

(BOTTOM) Table comparing the diurnal scaling factors with scaling factors derived from SSM/I data. Time-of-day effects are an important contribution to intersatellite differences. F10 is an outlier with known instrument problems. These scaling factors are not applied to the publicly available UMORA products (www.remss.com).



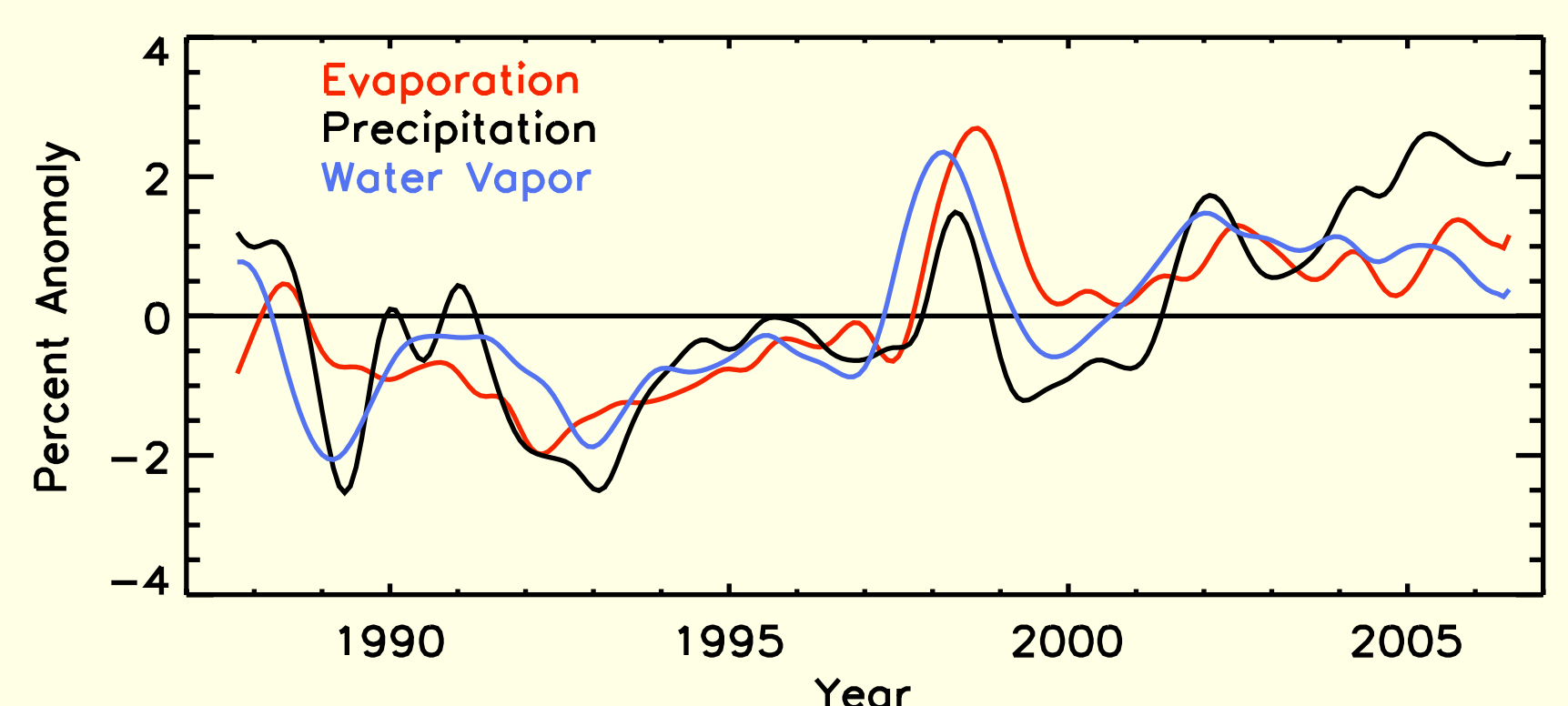
| Satellite | Diurnal Scaling | Scaling |
|-----------|-----------------|---------|
| F08 | 0.992 | 0.990 |
| F11 | 0.994 | 0.983 |
| F13 | 0.991 | 0.964 |
| F14 | 1.012 | 1.015 |
| F15 | 1.024 | 1.031 |
| F10 | 1.023 | 0.908 |



Agreement with GPCP and GPROF

(TOP) Time series of global-average annual rain rate anomalies from GPCP (black) and UMORA SSM/I (red). Note that GPCP is well correlated with UMORA after 1997, but the correlation between the time series is lower prior to 1997.

(BOTTOM) Time series of tropical-average (+20 to -20 deg) annual rain rate anomalies from GPCP (black), UMORA SSM/I (red), UMORA TMI (blue with asterisk), and GPROF TMI (green with triangle). TMI rain rates retrieved by UMORA and GPROF agree to within 1.2% on the average. The two algorithms still have considerable differences on storm scales.



Hydrological Consistency

(TOP) Anomaly time series of global-average precipitation and evaporation and over-ocean results for total water vapor. Water vapor is from UMORA. Evaporation has been calculated using UMORA wind speeds, Reynolds SST, an ICOADS climatology of relative humidity, an air-sea temperature climatology from the Hadley Center's nighttime marine air temperatures, and the bulk formula from the NCAR CAM 3.0. Land evaporation is assumed to be a static average value (note that 86% of evaporation is from the ocean). Precipitation over land is filled with GPCP. Using hydrological consistency as an indirect validation technique, it appears that the current version of UMORA rain rates are too low in the middle latitudes. A static, latitude-dependent adjustment has been applied for this analysis. The adjustment increases the global average rain rate by 18%. Reasons for this underestimation could be in UMORA's assumptions about the rain vertical profile or in its lack of sensitivity to frozen precipitation. The relative time lags between water vapor, precipitation, and evaporation are due to the strong relationships between SST and vapor and between evaporation and wind.

(BOTTOM) The table shows that global evaporation and precipitation match to 1%. The table also shows that the evaporation trends match the precipitation trends - as is required by hydrological balance. Our data shows that the precipitation trends are of the same magnitude as the water vapor trends. This is different than climate models, which predict a muted response by precipitation.

| Parameter | Mean | Std. Dev. | Trend |
|---------------|-------------|-----------|-------------|
| Evaporation | 961 mm/year | 1.1% | 1.3%/decade |
| Precipitation | 950 mm/year | 1.4% | 1.4%/decade |
| Water Vapor | 28.5 mm | 1.0% | 1.2%/decade |